Novel Quantum Dot-Ionogel Light Emitting Devices and a Determination of the Mechanism for Electroluminescence

An Honors Thesis for

The Department of Chemical and Biological Engineering

By

Jared Nash

Tufts University 2014

Acknowledgements

This thesis was made possible by many different individuals and groups. I want to first and foremost thank Professor Matthew Panzer for all of his support, guidance, and aid in performing this research. He has been generous with his time and his advice during this research has helped me immensely. I greatly appreciate all that he has done to help me complete this research. He has been a great mentor to me and has inspired me to become a better researcher. Of course, all of this research would not have been possible without the use of his laboratory either.

I am grateful to my academic advisor and committee member Professor Hyunmin Yi. Professor Yi has helped me greatly by suggesting I get involved in research early in my undergraduate career and helped me receive funding.

I want to thank all of the graduate students in Professor Panzer's laboratory for all their help. Adam Visentin, Ariel Horowitz, Changqiong Zhu, and Stephanie Flores helped me in getting my bearings in the laboratory and helped me with my laboratory skills. I also appreciated the time spent in group meetings helping me piece together all of the data into a coherent story.

I want to thank the Tufts Summer Scholars Program, QD Vision, and the Department of Chemical and Biological Engineering. With the generous and prestigious grant from the Summer Scholars program, I was able to begin this research project. I want to thank QD Vision for donating the quantum dots that were used in this research. I want to thank the members of the department with all of their help in obtaining the materials and all of the administrative matters that were associated with this project. Finally, I would like to thank all of my friends and family for all of their support and for helping me achieve my goals.

Table of Contents

List of Figures

List of Tables

Abstract

Colloidal quantum dots are an emerging class of nanomaterials beginning to be implemented into commercial displays. Companies such as Sony, QD Vision, and Apple are all currently researching quantum dot display technologies. Quantum dots are semiconducting nanoparticles that emit very saturated colors which make them ideal for displays. This research used colloidal quantum dots and a room temperature ionic liquid suspended in a polymer matrix (ionogel) to create a novel light emitting device architecture. The originally proposed mechanism for this device was to use the ionic liquid in the ionogel to create a large electric field around the quantum dots, causing the quantum dots to self-ionize and emit light. This new device architecture proved to be versatile, using both AC and DC biases. The peak wavelength of the electroluminescence was 612 nm and the emission spectra had a full width half peak of 30 nm; therefore, these devices emitted a saturated red color. The external quantum efficiency was calculated to be approximately 0.002%. These devices were operational in ambient conditions and were stable over a period of at least 3.5 hours. Because the devices were operational using a DC bias, the mechanism for electroluminescence could not be the originally proposed mechanism. Device functionality most likely involved a redox reaction with water vapor being one of the reactants. Future work should be performed to determine the reaction responsible for electroluminescence, and to improve the efficiency of light emission.

1. Introduction

1.1. Overview

Currently, light emitting devices (LEDs) are being touted as the future for display technologies[1]. LEDs can produce bright light with relatively long lifetimes and are considered to have better performance than other display technologies[1].

One main reason LEDs are not universally used is they are more expensive to produce than incandescent light bulbs[1]. The goal of an LED is to inject high energy electrons into an emissive layer, then let the electrons relax, emitting light. The final step is to remove the low energy electrons.

Currently, inorganic (non-carbon based) LEDs require very difficult processing in order to achieve the desired efficiency[1]. One technology that has shown some improvements is organic LEDs (OLEDs)[1]. OLEDs utilize an organic (carbon based) semiconductor as the emissive layer. OLEDs utilize cheaper fabrication techniques to reduce the processing cost. However, to achieve efficient devices, many different layers of materials are needed in order to inject electrons efficiently and use those electrons to emit light[1]. OLEDs also do not emit very saturated colors compared to inorganic LEDs[1]. Another emissive material that is gaining favor is quantum dots for their use in quantum dot LEDs (QD-LEDs)[2].

Quantum dots are nanoparticle semiconductors that can be tuned to emit highly saturated colors[3]. By simply changing the size of the quantum dot nanoparticle, a different color of light can be emitted[4]. A monodisperse quantum dot solution can then emit a highly saturated color[4]. Quantum dots also offer solution based fabrication processes such as spin coating, which can decrease the cost of production[1]. Quantum dots therefore offer a relatively low cost solution

processed material that can improve the color saturation of displays compared to LEDs and OLEDs[1].

There are currently companies that are researching the use of quantum dots for television displays[2]. Such companies are the well-established Sony and Apple as well as the newer QD Vision[2,5]. QD-LEDs are able to reduce cost by being solution processed, but currently, they still require the complex multiple layered structures similar to OLEDs. In order to get the efficient injection of electrons into the emissive layer, low work function metals such as aluminum or calcium are used as one of the electrodes[1,3]. Low work function metals are reactive which make them unstable in air. Because of the low work function electrode, QD-LEDs are often fabricated in nitrogen glove boxes[3]. If a QD-LED were to be used, it would need to be packaged tightly to ensure no oxygen entered the LED. One way to reduce cost would be to create a QD-LED that does not need to be encased in air-tight packaging.

1.2. Materials

The materials used in this investigation were indium tin oxide (ITO) transparent electrodes, quantum dots, toluene as a solvent for the quantum dots, room temperature ionic liquids, poly(ethylene glycol) diacrylate (M_n 575), 2-hydroxy-2-methylpropiophenone, gold, Spectracarb carbon fabric paper, and Marketech carbon nanofoam paper. The electrode touching the quantum dots was always a transparent ITO electrode. The other electrode in the fabricated devices was either ITO, gold, Spectracarb carbon fabric, or Marketech carbon nanofoam.

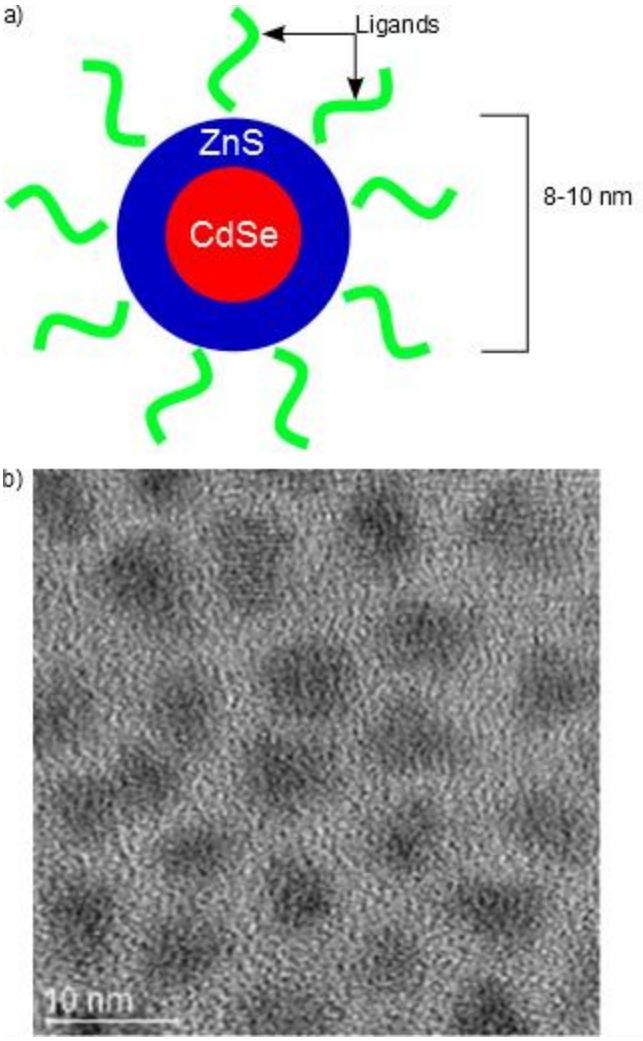

Figure 1.2.1 a) Single core-shell quantum dot. The core (CdSe) is surrounded by a shell (ZnS) in order to improve efficiency. This is the assumed composition of the quantum dots donated by QD Vision. b) TEM image of a quantum dot solution. The sizes of the quantum dots donated by QD Vision are 8-10 nm and the ligand lengths are 1-3 nm. Image courtesy of Dr. Anna Osherov.

For this study, a quantum dot solution was donated by QD Vision Inc. Even though the exact composition of the quantum dots is a trade secret, it was believed that the quantum dots were core-shell quantum dots. Core-shell quantum dots have fewer surface defects which helps improve their luminescence efficiency[6]. The core of the quantum dots was assumed to be cadmium selenide (CdSe) and the shell was assumed to be zinc sulfide (ZnS). The quantum dots were suspended in toluene. In the processing of quantum dots, ligands were added to the surface[7]. These ligands hindered coagulation and allowed the quantum dots to remain suspended in solution[7]. An estimation of the quantum dots composition was shown in Figure 1.2.1(a). Only one quantum dot size was utilized in this study. The size of the ligands were approximated as half of the distance between two adjacent quantum dots. From Figure 1.2.1(b), the actual quantum dot and ligand sizes were approximated as 10 nm and 2 nm, respectively. This size emitted red light, so all devices created in this research were red QD-LEDs.

The major room temperature ionic liquid that was investigated was 1-ethyl-3-methylimidazolium bis(trifluoromethylsulfonyl)imide (EMITFSI). The other room temperature ionic liquids were 1-ethyl-3-methylimidazolium tetracyanoborate, (EMITCB) and 1-ethyl-3-methylimidazolium tris(pentafluoroethyl)trifluorophosphate (EMIFAP). The structures of the ionic liquids were shown in Figure 1.2.2.

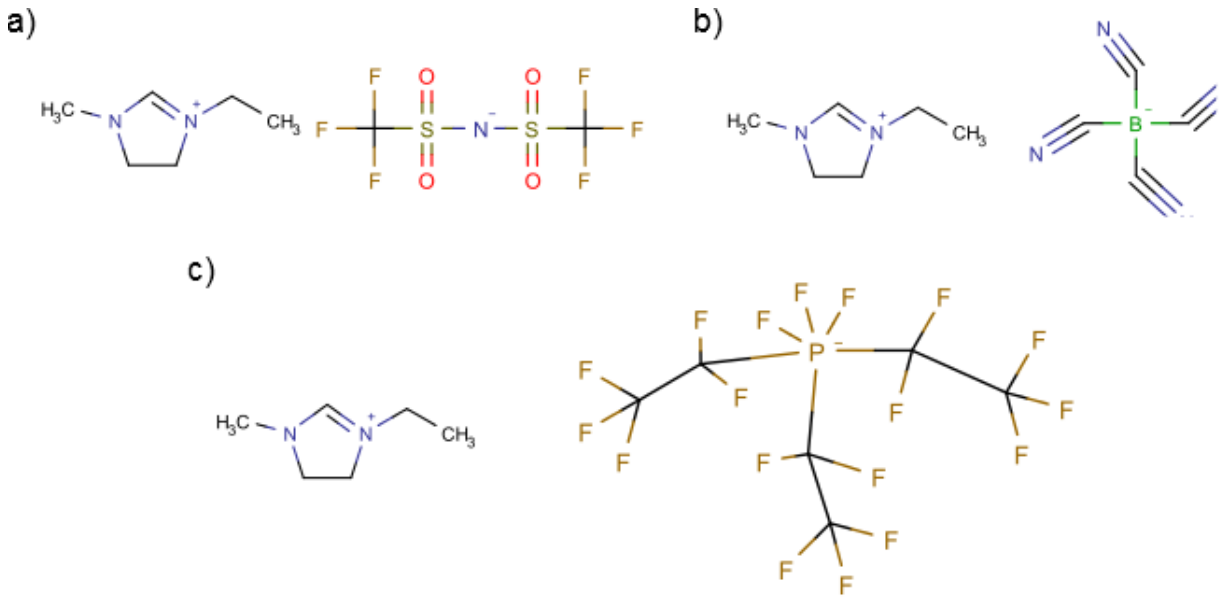

Figure 1.2.2. Chemical Structures of Three Ionic Liquids. a) EMITFSI b) EMITCB c) EMIFAP

Ionic liquids offer a large electrochemical window in which they can operate. A large electrochemical window means the ionic liquid is stable in a larger range of voltages compared to other solvents, such as water. With potentially large voltages needed for device operation, ionic liquids can increase the durability of the device. Because ionic liquids are salts that melt around room temperature, there are a large number of anions and cations moving around[8]. Due to a high ionic conductivity when an electric field is applied around an ionic liquid, the ions will align themselves to the applied field[9]. By moving to align to the electric field, the ionic liquid can maintain a large electric field around the quantum dots.

The original quantum dot solution was stored in a nitrogen glove box covered with foil to prevent photobleaching and photooxidation[10, 11]. Any quantum dot solution that was created and all other chemicals were stored in the dark under ambient conditions.

1.3. Background

The main focus of these devices is the quantum dot. As stated earlier, quantum dots are nanoparticles of a semiconducting material[3]. Semiconductor materials have an energy associated with them known as the band gap energy. The band gap energy of semiconductors determines the different energy levels that electrons can occupy.

The upper energy level is known as the conduction band and it has the lowest unoccupied molecular orbital (LUMO)[7]. The lower energy level is known as the valence band and it has the highest occupied molecular orbital (HOMO)[7]. The main design on an LED is to inject a high energy electron into the LUMO and remove electrons from the HOMO. By removing electrons from the HOMO, a hole is formed. A hole is the absence of an electron or a position in which an electron once was. Holes are not physical objects, but rather mental constructs to help explain the motion of electrons. When high energy electron in the LUMO pairs with a hole in the HOMO, an exciton is formed. Because the electron in the LUMO is in a high energy state, it can reduce its energy by recombining with the hole or relaxing down into the hole.

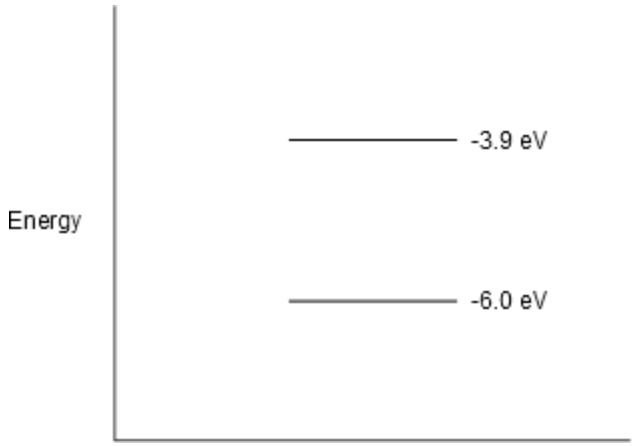

Figure 1.3.1. Energy Band Diagram of a Red CdSe ZnS Core-Shell Quantum Dot. The lower energy level is known as the valence band. The upper energy level is the conduction band. The energy values for each band were taken from reference [3].

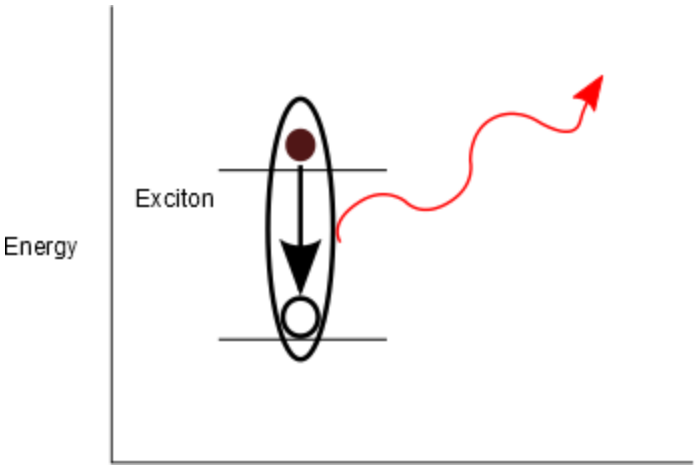

Figure 1.3.2. Exciton Relacation in a Quantum Dot. An electron in the conduction band relaxes into a hole in the valence band causing a photon of light to be emitted.

Upon recombination, a photon of light is emitted[1].

A photon of light being emitted by an electron recombining with a hole is known as radiative recombination[1]. When radiative recombination occurs, the color of light that is emitted is based on how much energy the photon has. What determines the energy of the photon is the energy difference between the HOMO and the LUMO[1]. By fine tuning the energy difference between the HOMO and LUMO, the color of the emitted light can be fine-tuned.

For quantum dots, much of this is true, but there is one distinct difference. For bulk materials, the band gap energy is a material property. When materials are created on the nanoscale, there are deviations from bulk material properties[3]. The major deviation can be explained through the particle in a box theory. Particle in a box is a setup where an electron is confined into a metaphorical box. Because the electron has some energy, it moves like a wave in the box[12]. Due to electrons' wave-like properties, the wavelength of the electron must be an integer multiple of the box length[12]. If the wavelength was not proportional to the box length, the electron would destructively interfere with itself and change its energy. Because the box is a finite length, the wavelengths that the electron can move in are quantized. Because the wavelength the electron moves with is directly proportional to the energy of the electron, the electron can only occupy certain energy states[12,13]. From quantum mechanics, it can be proven that the separation between energy states decreases as the length of the box increases[12, 13]. This

means the larger the box, the smaller the difference between the HOMO and LUMO. In a bulk material, there is no metaphorical box so there is no quantization of the energy levels[13]. This box for quantum dots is the diameter of the nanoparticle. This is how quantum dots can be tuned to emit certain colors and why a quantum dot's size determines its color. The larger the box, the smaller the energy difference between the HOMO and LUMO; the larger wavelength of light emitted, the redder the color. If the quantum dot is very small, the shorter the wavelength of light emitted, the bluer the color. The quantum dots used in this research were relatively large because they emitted a red color. With the quantum dots having a core-shell structure, the percentage of excitons that undergo radiative recombination increased compared to just quantum dots without shells.

The next interesting component of these devices is the ionogel. Ionogels are room temperature ionic liquids suspended in a polymer matrix. As noted earlier, ionic liquids are made entirely of ions and are liquid at room temperature[9]. Ionic liquids also have negligible vapor pressure which means the ionic liquid should not evaporate[8]. Because they have no vapor pressure, they can be suspended in a polymer matrix and maintained in the matrix without evaporating. The ions are mobile and can align to an electric field[9]. This forms a capacitive layer, creating a large electric field over a relatively short distance[9]. Because of the large electrochemical window, a large electric field can be applied without the ionic liquid decomposing. By suspending the ionic liquid in a gel, the gel is able to retain much of the electrochemical properties of the ionic liquid, but in a solid state device[9].

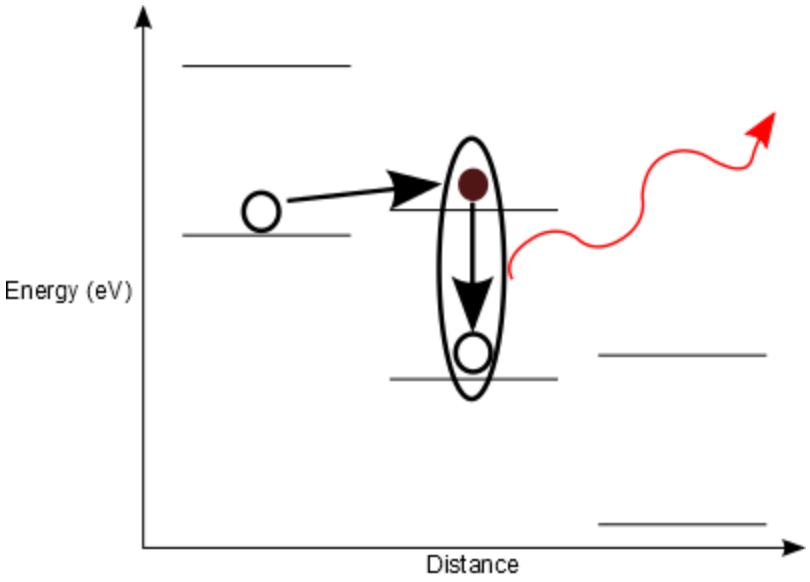

Figure 1.3.3. Self-Ionization Mechanism. An electron moves from the valence band in one quantum dot to the conduction band in an adjacent quantum dot, leaving a hole. When an exciton forms on a quantum dot, the electron can radiatively recombine and emit a photon of light.

For this research, the general device architecture was based off previous research in which a large electrical potential was placed around a quantum dot layer[7]. It was shown that quantum dots can shift their average energy levels with a large enough electric[7]. The shifting of the energy levels affects the position of the conduction band and the valence band[7]. Because all of the quantum dots do not feel the same electric field, the quantum dot energy levels shift relative to each other[7]. When a large enough voltage is applied, one quantum dot's conduction band energy becomes higher than an adjacent quantum dot's valence band energy[7]. An electron from the higher energy conduction band can move to the lower energy valence band[7]. If there is a hole on the second quantum dot, an exciton forms[7]. If the electron relaxes back down into the hole, a photon of light is emitted[7]. This phenomenon was denoted as self-ionization[7].

Because there is a limit to the number of electrons in a quantum dot thin film, to get sustained light, the polarity of the electric field would need to be reversed. This limits the device to only applications with an AC bias[7]. Theoretically, there would be no injection of electrons into the quantum dots. This was the theoretical mechanism for the novel device design.

In the novel device structure, a large electric field would be applied to the device and the ions in the ionic liquid would align to the electric field. When the ions align, the quantum dots would experience a large electric field. When a large enough field was applied, the quantum dots would self-ionize. The polarity of the electric field would need to switch constantly in order to get sustained light emission. With the large electrochemical window of the ionogel, the ionogel should have been stable and not degraded too quickly. By making the ionic liquid into an ionogel, the entire device can be solid state.

1.4. State of the Art for QD-LEDs

The current technology for QD-LEDs is, in general, an OLED with a layer of quantum dots in the middle[4]. With this structure, electrons must be injected into the quantum dot layer in order to get light emission[4]. The quantum dots need to be placed in a very specific manner in order to achieve the maximum efficiency[1]. Generally, QD-LEDs have a monolayer of quantum dots[7]. It is worth noting however that the QD-LEDs that utilized the self-ionization mechanism required multiple layers of quantum dots[7].

1.5. Objectives

The objective of this research was to create a novel device structure with a quantum dot thin film, an ionogel, and two electrodes. If this device structure was functional, the two secondary objectives were to determine the mechanism for luminescence and to determine the stability of the device.

2. Experimental Methods

2.1 QD Solution Preparation

The donated quantum dot solution was stored in a nitrogen filled glove box in a sealed container to ensure that there was no photoxidation of the quantum dots[11]. The solution was also covered in order to limit light exposure, which could have caused the quantum dots to photobleach and lose their color[10]. A small aliquot was removed from the glove box when needed. The aliquot was then diluted by adding anhydrous toluene to the aliquot that was removed from the nitrogen glove box. The dilution was about four units of toluene to one unit of the donated quantum dot solution.

2.2 Gel Precursor Solution Preparation

The gel precursor solution was made by combining the room temperature ionic liquid with a poly(ethylene glycol) diacrylate (M_n 575) (PEGDA) and 2-hydroxy-2-methylpropiophenone (HOMPP). The ionic liquids were purchased from EMD Chemicals Inc. The PEGDA and HOMPP were purchased from Sigma Aldrich. The PEGDA was the polymer that created the matrix that held the room temperature ionic liquid in the gel. The HOMPP is a UV initiator that was used to initiate the polymerization. Most of the precursor solution was created at a weight percent of 8.2% PEGDA, 2% HOMPP, and 89.8% room temperature ionic liquid. 1 mL of the solution was prepared at a time because if the solution was left standing for too long, the HOMPP initiated the polymerization of the PEGDA solution even without direct UV curing.

2.3 ITO Cleaning

Glass substrates coated with a thin layer of ITO were manufactured and purchased in large quantities (Thin Film Devices Inc.). In a four stage process, these substrates were cleaned in order to achieve an even film deposition. The first process was a soap solution cleaning. The substrates were placed in a Teflon holder and then submerged in a 2% Micro 90 soap solution (Sigma Aldrich) which was contained in a beaker designated for the soap solution. The beaker was then placed in an ultrasonicator for 5 minutes. The Teflon holder with the substrates was submerged in a deionized water solution that was created with in-house deionized water. The substrates were then placed in the ultrasonicator for 5 minutes. The third step was to put the substrates in a laboratory grade acetone (Fischer Scientific) solution in the ultrasonicator for 5 minutes. The final step was to place the substrates into a boiling laboratory isopropanol (Fischer Scientific) bath for 5 minutes. The substrates were then dried off by flowing nitrogen gas and were placed ITO side down in polypropylene holding cases (Entegris Inc.).

2.4 Spin Coating a QD Thin Film

Quantum dot thin films were created by spin coating. The substrate was placed onto a chuck in the spin coater. Vacuum was drawn on one side of the substrate in order to stabilize it to the chuck. The quantum dot solution was deposited by a disposable syringe and a 0.45μm PTFE filter (Millipore). Enough quantum dot solution was deposited to cover the entire

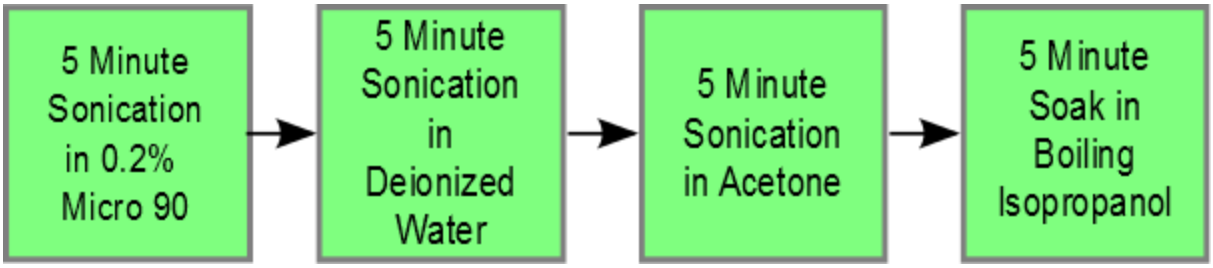

Figure 2.3.1. Cleaning Treatment Flow Chart.

substrate. The solution and substrate were spun using a Laurell Technologies spin-coater (WS-400BZ-6NPP/LITE) for one minute. The majority of films were created with a spin speed of 1000 rpm because that speed gave the thickest uniform coating, but some were spun at 2000 rpm and 3000 rpm. After removing the substrate from the spin coater, it was returned to the case and left to dry for a few minutes in the fume hood. After drying, the substrate was placed face down in a case to preserve the thin coating of quantum dots.

2.5 Sandwich Device Fabrication

The sandwich setup was made by stacking an electrode, a quantum dot layer, an ionogel and another electrode into a device.

There were different sandwich setups that differed in how the ionogel was fabricated. The procedure for ionogel curing was the same procedure that was described by Visentin and Panzer[7]. The first ionogel was created by placing a Teflon cylindrical mold on a cleaned ITO glass backed substrate, placing the precursor solution in the mold, and curing the solution under 365 nm longwave UV radiation (Spectronics Corp., 8 W) for two minutes to cross link the acrylate functional groups[7]. The device was then left in ambient conditions for a few hours to allow any volatile compounds in the gel to evaporate. A two minute curing time was sufficient to create a stationary solid gel. The ionogel and ITO glass backed substrate were then compressed together using paper clips, which did not always provide reliable

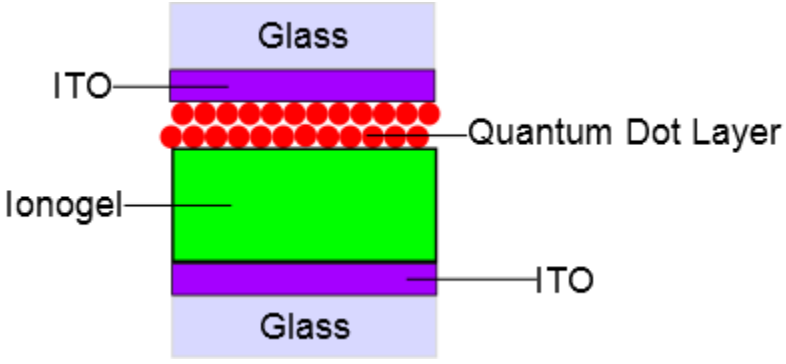

Figure 2.5.1. Sandwich Architecture. Quantum dot layer was spin coated on ITO. Ionogel was sandwiched between the quantum dot layer and the other electrode. Figure not drawn to scale.

contact between the electrodes and the ionogel. The first variation on this setup was removing the Teflon mold after the ionogel was cured. In order to maintain structural integrity in this design, small spacers were placed to the sides of the ionogel. The next variation was replacing the ITO glass backed substrate with a piece of carbon paper attached to a glass substrate. The third variation was taping the sides of a quantum dot coated ITO glass backed substrate, placing the precursor solution in between the tape, then using a razor blade, smooth the gel precursor solution to an even height. After creating the desired gel height, the gel was cured and then the counter electrode was placed on top of the gel. This created a smaller separation between the electrodes which was thought to help create a larger electric field around the quantum dots.

2.6 Coplanar Device Fabrication

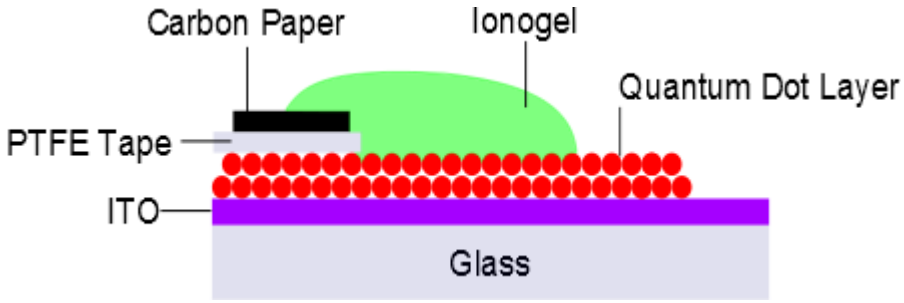

Figure 2.6.1. Coplanar Architecture. A quantum dot layer was spin coated onto ITO. A piece of PTFE tape was used to prevent contact between the electrodes. The ionogel was cured to provide contact between the carbon paper and the quantum dot layer. Figure not drawn to scale.

The coplanar setup was created to make the emitted light more visible. This setup involved taping one end of a quantum dot covered ITO with Teflon tape to act as an insulator.

A small piece of carbon paper was attached to the Teflon tape. The ionic liquid precursor solution was then pipetted onto the top of the device making sure to bridge the gap between the carbon paper and the quantum dot layer. The precursor solution was cured in the exact same conditions described above in the Sandwich Device Fabrication. The one variation for the

coplanar architecture was placing tape along the sides of the quantum dot covered substrate and, using a razor blade to smooth out the gel to a smaller height. This gave a slightly more repeatable geometry, but also gave a smaller gel thickness.

2.7 Neat Ionic Liquid Device Fabrication

A piece of ITO on PET was cleaned by rinsing the substrate with deionized water, acetone, and isopropanol. The piece was then coated with the quantum dot solution by spin coating. The quantum dot covered ITO on PET was then cut into a smaller piece. A small piece of carbon paper was also cut out in order to be able to fit the two into a small beaker. Ionic liquid was then placed into a small beaker with the carbon paper and the quantum dot covered ITO. A diagram can be seen in Figure 2.7.1.

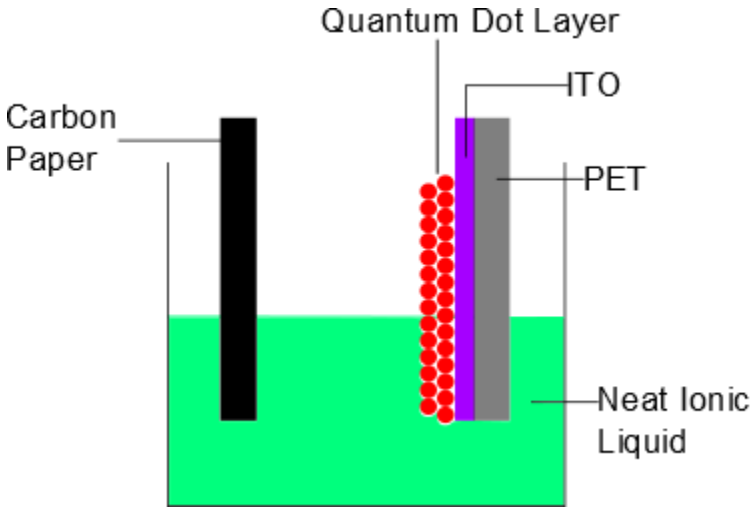

Figure 2.7.1. Neat Ionic Liquid Device Architecture. A quantum dot layer was spin coated onto an ITO on PET substrate. The ITO covered substrate and a piece of carbon paper were dipped into a beaker with neat ionic liquid.

2.8 Hydrogel Device Fabrication

A hydrogel was also tested to see if the ionic liquid was a necessary component. The hydrogel solution was prepared the same way as the ionogel solution except the ionic liquid was

replaced by water. The hydrogel precursor solution was made by combining deionized water with the PEGDA and HOMPP. Most of the precursor solution was created at a weight percent of 8.2% PEGDA, 2% HOMPP, and 89.8% deionized water. 1 mL of the solution was prepared at a time and the curing was performed as described in Sandwich Device Fabrication above. . A few of the hydrogels were soaked in different solutions in order to test different environments. After curing, the hydrogel was placed in either a 0.25M NaOH or a 0.01M NaCl solution and left to soak overnight. These hydrogels were then placed into sandwich device architectures for testing.

2.9 Performance Characterization

Testing of these devices was conducted in both DC and AC biases. The majority of AC bias testing was focused on the turn-on voltage, emission spectrum, and stability in air.

For the AC bias testing, an AC bias was applied by an Instek GFG-8250A function generator at increasing voltages until light emission was first seen. The voltages at which light emission was first seen were usually close to 6 V PTP.

For the stability testing, the device was manually set up above a Thorlabs S120VC photodiode detector in order to record the power of the light output from the device.

For DC bias testing, a Kiethley 2602A System Sourcemeter applied a variable voltage until light emission was first seen. The majority of testing occurred with the non-quantum dot electrode being the positive electrode and the quantum dot covered ITO electrode being the negative electrode.

The spectroscopy of the electroluminescence and the photoluminescence were determined using an Ocean Optics Spectrophotometer USB4000. The photoluminescence of the device was created using a small handheld 4 watt black light.

Even though quantum dot film thicknesses were not determined to be an absolutely critical part of this investigation, atomic force microscopy (AFM) was used to determine the thicknesses of the quantum dot spun layer. The quantum dot layer was spun onto an ITO on glass substrate. The film was scratched with a pair of tweezers and the depth of the scratch was determined to be the thickness of the quantum dot film. The thickness was then compared to the turn-on voltages and the results can be seen in Appendix A.

2.10 Mechanism Determination

The majority of testing in DC bias was focused on determining the mechanism for electroluminescence. The majority of the testing occurred in ambient conditions.

In order to determine the mechanism for electroluminescence, devices were tested in different chemical environments. The first was in a nitrogen glove box. The second test entailed exposing a device created in ambient conditions to steam. The device was turned on by applying the necessary voltage. Deionized water was then boiled in a small beaker, which was then transferred to the lab bench and the functioning device was exposed to any vapor above the boiling water. The response of the electroluminescence to the vapor was observed. The final condition was a carbon dioxide enriched environment. A device was created in ambient conditions. The device was turned on by applying the necessary voltage. Dry ice was sublimed in a container with a small hose that was clamped shut. Once pressure built up, the clamp was removed and the hose was placed over the device. The response of the electroluminescence to the carbon dioxide was observed.

2.11 Data Analysis

The external quantum efficiency was determined using equation E-1.

$$EQE\% = \frac{W * \frac{\lambda}{hc}}{i * \frac{N_{av}}{F}} * 100 \quad \text{(E-1)}$$

W - Luminous power at current, i (J/s)
λ - Wavelength of light emitted (612 nm)
h - Planck's Constant ($6.626*10^{-34}$ J*s)
c - Speed of Light ($3.00*10^{8}$ m/s)
i - Current through the device (C/s)
N_{av} - Avogadro's Number ($6.022*10^{23}$ 1/mol)
F - Faraday's Constant (96485 C/mol)

The raw data of the spectra of the electroluminescence and the photoluminescence were each fit to a Gaussian function. The fitted functions were then normalized to one in order to plot them in the same graph. From the normalized emission spectra, the peak wavelength and full width half peak values were determined.

3. Results and Discussion

3.1 Devices

All device structures were functional and emitted light. The luminescence for the majority of the devices was seen at the triple interface between the quantum dot layer, the ionogel layer and air, but there were some devices that did show luminescence at the quantum dot ionogel interface.

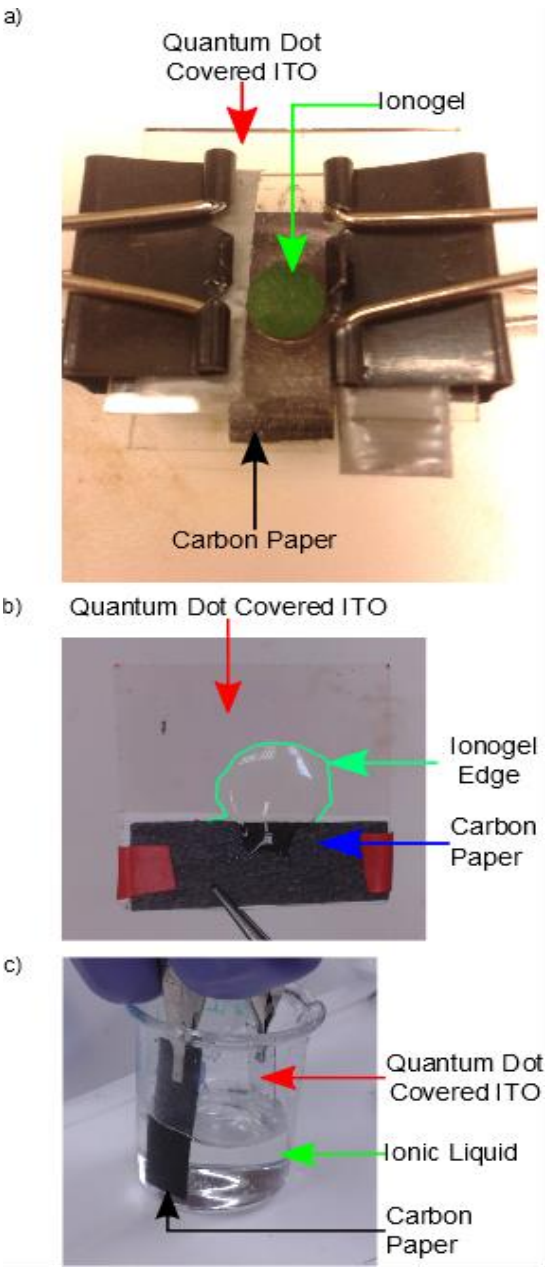

Figure 3.1.1. Pictures of Device Architectures. a) Sandwich device architecture. b) Coplanar device architecture. c) Neat ionic liquid device architecture.

The sandwich device architecture seen in Figure 3.1.1(a) had the most well-defined quantum dot, ionogel interface and was the most repeatable geometry. With electroluminescence being limited to the triple interface, this structure was not as useful because the triple interface was relatively small. With the sandwich setup, the emitted light had to pass through a second transparent electrode and glass, making characterization more difficult.

The coplanar setup formed the best device for characterization because a larger number of coplanar devices demonstrated uniform light emission at the quantum dot, ionogel interface.

The brightest portion of the coplanar devices was still at the triple interface. These devices did not have the second electrode impeding light emission, which made it better for characterization. However, they were not able to create repeatable triple interface geometries.

The neat ionic liquid device showed even more emission at the quantum dot, ionic liquid interface when compared to the coplanar device, but the brightest part of the pixel remained at the triple interface. This structure was useful in order to make sure that the PEGDA and the HOMPP were not involved in the electroluminescence. More testing about the effect of different ionic liquids and the PEGDA and HOMPP can be seen in Appendix B.

3.2 Electroluminescence Characterization

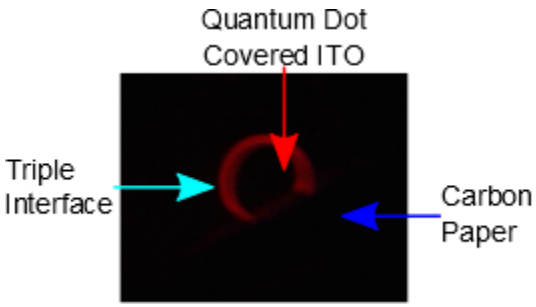

Figure 3.2.1. Coplanar Device Light Emission. The emission seen here is limited to the triple interface between the quantum dot layer, the ionogel, and air.

As stated above, all three device structures were functional and showed electroluminescence, as seen in Figure 3.2.1. The first devices were tested using an AC bias because the proposed mechanism would not function with a DC bias. After looking closely at the device functioning, it was noted that the device only showed electroluminescence either at the peaks or the troughs of the AC bias depending on the how the device was connected to the function generator. It was determined that not only was the voltage important to device performance, but also polarity. The quantum dot covered ITO electrode needed to be the negative electrode in order for the device to function. If the proposed mechanism was correct, the device would have showed electroluminescence at both the peak and the trough of the applied AC bias. Because electroluminescence was only seen at the peaks or troughs, it was

determined that the device was only functioning after a certain voltage was reached. Devices were then tested using DC biases and, being function, the mechanism for luminescence could not have been the proposed mechanism. The majority of devices were functional when a 3.5 V DC bias was applied to them. With the devices functioning with DC biases and the majority of light emission being limited to the triple interface, a better understanding of what the triple interface looked like was determined.

The triple interface and the light emission were seen more clearly in the fluorescent microscope images seen in Figure 3.2.2. More images of the ionogel, triple interface were seen in Appendix C. The interface appeared to be affected by device operation. At the triple interface, small droplets formed. After watching a functional device under the fluorescent microscope, the droplets appeared to be small pieces of ionogel that had become detached from the main ionogel at the interface. The droplets did not appear to affect the performance of the device, but may have helped thin the ionogel. Such results led to the conclusion that a thinner ionogel layer, the more contact between air, quantum dots and ionogel which created a larger triple interface.

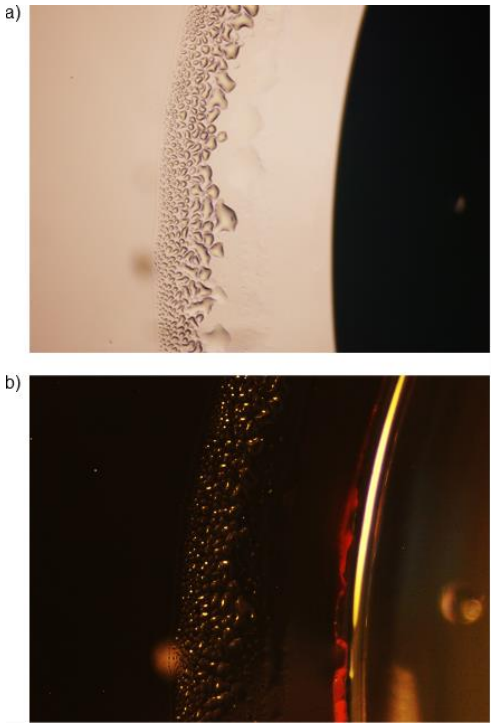

Figure 3.2.2. Fluorescent Microscope Images of a Coplanar Device. These images were taken aat 4X magnification. a) The device with no voltage being applied. b) The devive with a 3.3 V DC bias. The contrast and brightness of image (b) were increased to be able to see where the luminescence originated from.

Because the majority of the light was seen only at the edges, the device did not appear to be very efficient. In order to quantify how efficiently the device was functioning, the external quantum efficiency was

determined to have been 0.002%. This was most likely an underestimate of the actual external quantum efficiency because the photodetector was not able to detect all of the light emitted, but all of the current being supplied to the device was measured.

Even though this was most likely an underestimate of the external quantum efficiency, the external quantum efficiency was still most likely within one or two orders of magnitude of this value which means these devices were not very efficient.

The next important characterization was the electroluminescence spectra. The electroluminescence of the device was determined and was shown in Figure 3.2.3. In order to achieve a baseline of 0 intensity, the average intensity from the raw data in 500-550 nm range was removed from all of the data points. This data was then fit to a Gaussian curve using Matlab. The Gaussian fits were then normalized by dividing all points by the maximum of the fit. The emission spectra showed that there was a very small shift in the peak emission between photoluminescence and electroluminescence. This was uncommon because a larger peak shift for electroluminescence due to defects in the surface of the quantum dot was expected[14]. With surface defects, the energy difference between the HOMO and LUMO would have been decreased which would have caused a lower energy photon to be emitted. That there was no redshift suggested that the quantum dots used in these devices had minimal surface defects. The other interesting note was that the full width half peaks (FWHP) of the two spectra were almost identical. The actual peak position and FWHP values were shown in Table 3.2.1. The FWHP data also demonstrated that the quantum dots had very little surface defects and that the color was a saturated red color. By being able to use quantum dots, a better display could have been created because there can be little to no redshift in the electroluminescence, and the color can be highly saturated.

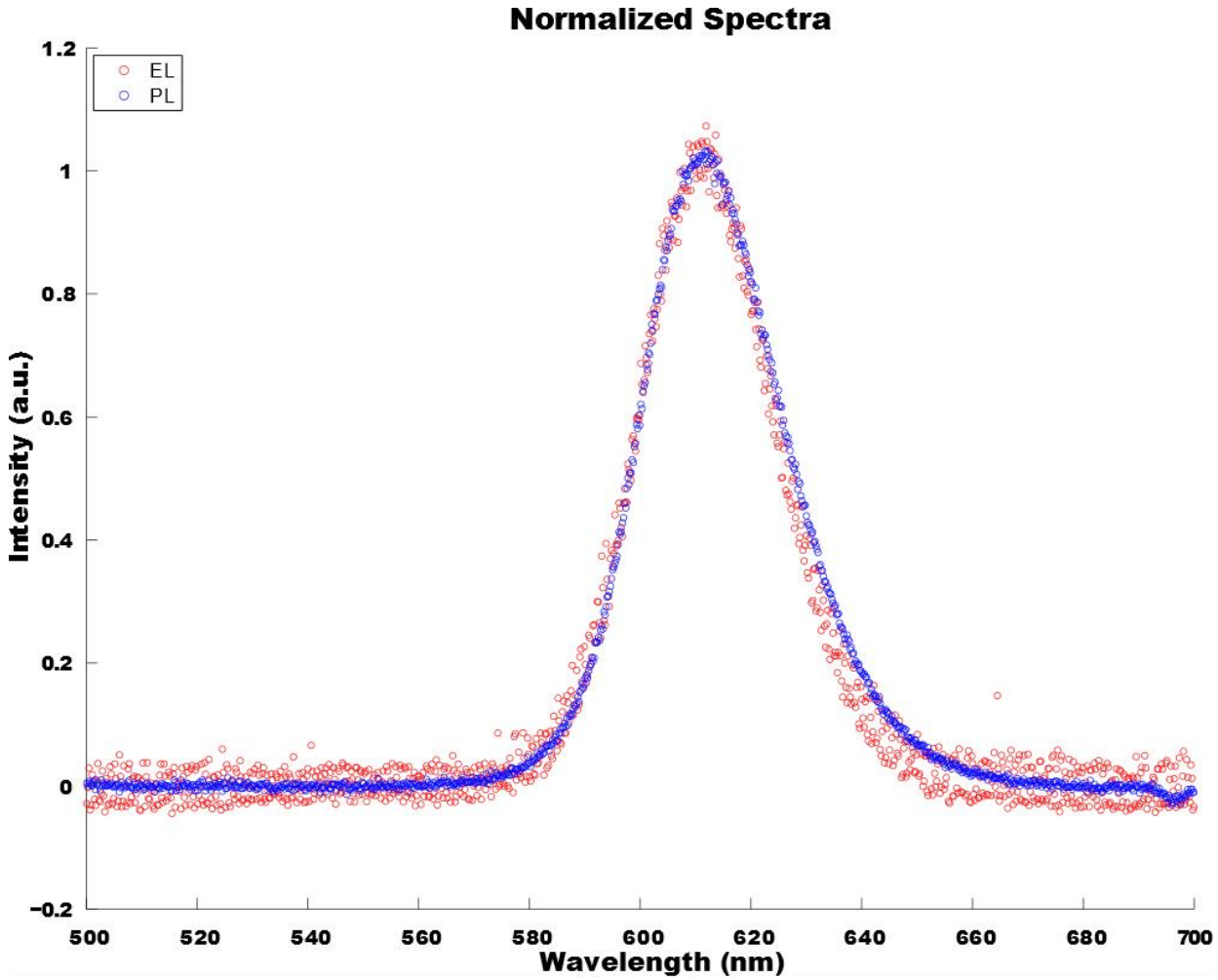

Figure 3.2.3. Normalized Electroluminescence and Photoluminescence Spectra. The average intensity from 500-550 for each spectrum was subtracted out to give a baseline of 0. Each spectrum with the adjusted baseline was then fit to a single term Gaussian function. Each spectrum was then normalized by the maximum of the fitted curve. The peak positions for each spectra were taken from the fits.

Table 3.2.1. Emission Characterization.

	Peak Wavelength (nm)	FWHP (nm)
Photoluminescence	613	31
Electroluminescence	612	30

Another characteristic of an LED that was observed was device performance at higher frequencies. Electroluminescence was seen at frequencies larger than 0.5 Hz, but the voltages required to achieve electroluminescence were significantly larger. This demonstrated that the device performed better at lower frequencies. This was in agreement with the observations that

the electroluminescence was only seen once a threshold voltage was achieved. The faster the frequency, the less time the voltage exceeded the threshold voltage.

With all of these tests performed in ambient conditions, the devices were proving to be relatively air stable. In order to get a more quantitative analysis of the stability, a 3.5 V DC offset with a 1 V PTP 0.5 Hz AC bias was applied to the device and the device was setup above a photodetector and left for 3.25 hours.

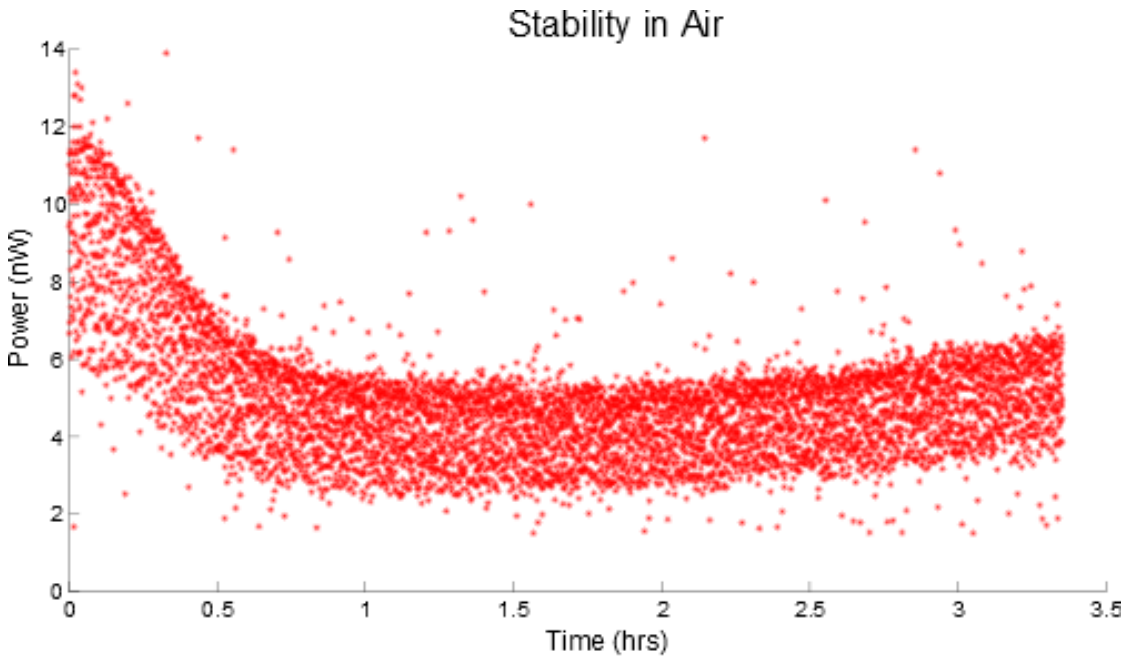

Figure 3.2.4. LED Stability in Air. A device was placed over a photodetector and a 3.5 V DC offset with a 1 V PTP 0.5 Hz AC bias was applied to a LED.

After testing, a baseline of 2 nW was offset from the data to ensure the off position was at a power of 0 nW. All non-peak points were then removed to give better clarity of the devices on and off states. After subtracting the baseline, all of the data points that were below 2 nW were determined to be data points from the device in the "off" state and were subsequently removed. Figure 3.2.4 presented the peak intensities observed by the photodetector during device operation. The reason there was a band of peak intensities was due to the photodetector

sampling the intensity three times per second. With a 0.5 Hz AC bias being applied to the device, one complete wave took two seconds. Because the polarity of the bias was important, only about one second was spent with the correct polarity on the device. Because the sampling rate and the time the device was functioning did not align properly, there was a range of peak intensities observed. The band of peaks shown in Figure 3.2.4 was attributed to the difference in timing between the sampling rate and applied bias. The LED did have a reduced electroluminescence after the first half an hour, but the device appeared to be stable for the rest of the testing as seen in Figure 3.2.4. It appeared that the device had slightly improved performance at 3 hours compared to 1 hour. This demonstrated that these devices were stable in air and did not need airtight packaging.

These tests verified the hypothesis that an air stable, solution based, quantum dot ionogel LED could be created. The device performance was in agreement with the literature that quantum dots emitted saturated colors and also showed that quantum dots could be processed to have almost no surface defects. The other interesting note was the device mechanism. The observations could not have been explained by the proposed mechanism which suggested that electroluminescence was not achieved by self-ionization of the quantum dots, but rather by a different mechanism that did not appear to have been previously described in the literature.

3.3 Gaseous Species Involved

Due to the device functioning with a DC bias, the mechanism was suggested to be an oxidation reduction (redox) reaction. In order to determine the redox reaction, device performance in a nitrogen environment was determined. Nitrogen is an inert gas which limited the amount of possible reactants present in the device. After creating an entire device in a nitrogen glove box, the device was tested with an AC bias. At the same voltages that previous

devices had been functional at, the device created in the nitrogen glove box did not function. When the same device was removed from the glove box and tested, it was functional. This result in conjunction with the stability data demonstrated that the device was not only stable in air, but actually required some component of air for electroluminescence.

Because electroluminescence was seen in ambient conditions and not in a nitrogen environment, a redox reaction was the most likely mechanism that involved one of the other gases in air. This significantly limited the available reactants to essentially carbon dioxide, oxygen, and water. Because no safe procedure for an oxygen-rich environment was determined, cyclic voltammetry (CV) was used to test for the possibility of oxygen being present and possibly involved in the reaction. The results of the CV testing were presented in Appendix D. The testing environments were then limited to carbon dioxide-rich and water-rich environments.

Carbon dioxide testing showed no noticeable change to device performance. This was surprising because theoretically, saturating the device with carbon dioxide should have produced some change in device performance. If the carbon dioxide was directly involved in the reaction, increasing the amount of carbon dioxide around the device should have improved the performance of the device and caused increased electroluminescence. If carbon dioxide was not involved in the reaction, the carbon dioxide should have displaced any other gas. By displacing any other gas, the carbon dioxide should have been the only gas at the triple interface, and the devices performance should have noticeably decreased. One explanation for no change in device performance during the carbon dioxide test was that the conditions for testing were not controlled as well as perceived and that the carbon dioxide did not entirely displace the other reactants. Because performance was not improved, carbon dioxide was thought to be an inert gas.

The first testing done to create a water-rich environment was to boil deionized water in a small beaker and then observe any difference in electroluminescence. Through this test, devices showed significant improvement in performance. When exposed, the luminescence increased dramatically in an almost instantaneous fashion. The second testing was to apply a voltage to a device that was just below the point of visible electroluminescence and then rotate the device over boiling water. This showed a drastic improvement in electroluminescence. More testing was done on the effect of the heat of the steam on device performance and was shown in Appendix E. These suggested that water was most likely a key component in the redox reaction. There was the possibility that dissolved oxygen or carbon dioxide could have been released, causing the increased luminescence.

In order to get a better sense of the vapor composition to which the devices were exposed, the amount of carbon dioxide, and oxygen at 20 °C and 40 °C were approximated. The volume of deionized water was approximately 20 mL. After a literature search, the mole fraction of carbon dioxide in water was found to be 0.0007 at 20 °C, and 0.0003 at 40 °C[15]. In order to calculate the amount of carbon dioxide in 20 mL of water, the moles of 20 mL of water was determined. By multiplying the volume by the density (1 g/mL) and dividing by the molar mass (18 g/mol), the moles of water was determined to be 1.1 moles. The moles of carbon dioxide were calculated by multiplying the corresponding mole fraction with the moles of water. This calculation works under the assumption that the moles of any dissolved species was negligible when compared with the moles of water. The solubility of oxygen in water was found to be 0.045 g/kg H_2O at 20 °C, and 0.031 g/kg H_2O at 40 °C[16]. Again, using 20 mL of water with a density of 1 g/mL, the grams of water were determined. By multiplying the grams of water by the solubility of oxygen, the grams of dissolved oxygen were determined. The grams were then

converted to moles by dividing the mass by the molar mass of oxygen which was approximated as 32 g/mol. The approximated amounts of gases in 20 mL of water were shown in Table 3.3.1.

Table 3.3.1. Approximated mMoles in 20 mL of H_2O.

Compound	**mMoles 20 °C**	**mMoles 40 °C**
CO_2	0.78	0.33
O_2	0.025	0.021
H_2O	1100	1100

As shown in Table 3.3.1, the amount of carbon dioxide and oxygen that were soluble in water at 20°C were very small when compared to the moles of water. This meant the assumption used to calculate the moles of carbon dioxide was a valid assumption. This data also showed that most of the vapor coming off of the deionized water was water vapor and not oxygen and carbon dioxide.

All of this suggested that water was the key component in the redox reaction for electroluminescence. The other question raised was with the role of the ionic liquid in these devices. If water was a key reactant, did the ionic liquid play any role at all? The voltages that were applied to the devices were larger than the voltage required to split water, so it was possible that the ionic liquid was simply another inert component.

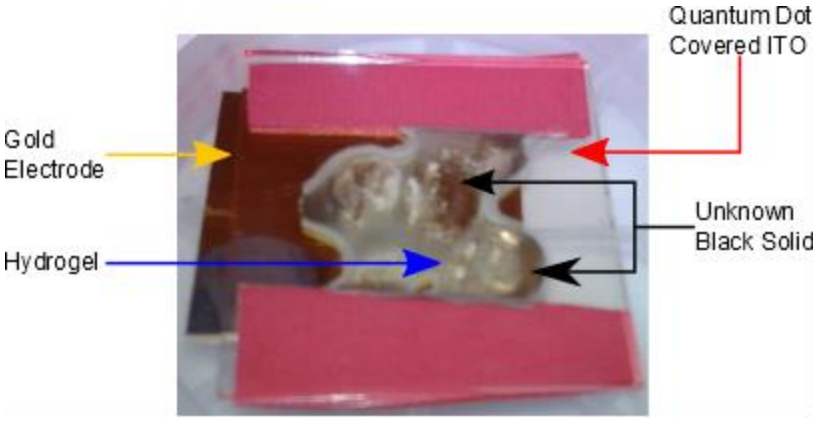

Figure 3.4.1. Hydrogel LED after testing. This device showed electroluminescence, but only after the black solid formed.

3.4 Hydrogel Performance

Since the data suggested that water was playing a critical role in electroluminescence, it

was assumed that using a hydrogel could improve the device performance drastically.

The hydrogel LEDs demonstrated electroluminescence, but there was no significant change in the performance compared to the ionic liquid gels. The electroluminescence was still limited to the triple interface between the air, the hydrogel, and the quantum dots. The other important note was that electroluminescence was only seen after a black solid formed. That there was no improved performance for the hydrogel devices did not agree with the deionized water testing. If water was the key factor in electroluminescence, then the interface between the hydrogel and the quantum dots should have showed electroluminescence, creating a more uniform pixel. If water vapor was the necessary component, a hydrogel should have produced more water vapor at the triple interface. Increased water vapor improved electroluminescence with the boiling deionized water experiment. That the device showed no improved electroluminescence suggested that the ionic liquid could mediate the redox reaction. The discoloration of the hydrogel also occurred at a much lower voltage than the ionogels. It is worth noting that the acidity of the water in the hydrogel did not change the device performance. When a hydrogel was soaked in a salt solution, the hydrogel was functional at lower voltages, but this was attributed to the improved conductivity of the salt soaked hydrogel compared to the deionized water hydrogel. This data pointed to water vapor being a key component. Even though devices performance was not increased by the hydrogel, devices were still able to function which suggests that water was likely a key factor, but only when it was in the vapor phase. This also pointed out that the ionic liquid may have stabilized the reaction. By stabilizing the reaction, the ionogel can function for a longer period of time without noticeable discoloration or affect to device performance.

4. Conclusion

This research demonstrated that a LED was created with quantum dots and ionogels. The devices had very few layers and were fabricated using solution based techniques. This could help make scale-up easier and cheaper. These devices showed electroluminescence with a very small shift in peak position between photoluminescence and electroluminescence while maintaining the color saturation. The stability of these QD-LEDs was determined to at least 3.5 hours in ambient conditions. The external quantum efficiency was low at approximately 0.002%. The mechanism for electroluminescence was not the hypothesized mechanism, but rather a redox reaction. This reaction appeared to involve water vapor as a necessary component, but more research needed to be conducted to conclusively determine the mechanism. If a concrete mechanism was determined, it might be possible to engineer an architecture that improves the efficiency.

5. Future Work

The research on this device could use further study in order to shed some light on some of the observations. The main example would be the improved electroluminescence in the presence of water vapor, but no increased electroluminescence when the ionogel was replaced with a hydrogel. With that in mind, the main focus could be on determining the exact mechanism for electroluminescence. One example of a future test would be observing how the device performs in an oxygen rich environment. If oxygen, not water, was the limiting reactant, it would explain why there was no increased electroluminescence from the devices made with a hydrogel.

Other future work would be to improve the external quantum efficiency. Without knowing the exact mechanism, it is difficult to say what exactly would improve the external quantum efficiency. One way to do this might be to make a uniform pixel. If diffusion of a gas is the limiting step, creating an extremely thin ionogel layer or an ionogel that is saturated with the limiting reactant could improve device performance.

One final possible future work could be the ionic liquid. The ionic liquids in this study all utilized the EMI cation. Other ionic liquids could mediate the redox reaction better than the ionic liquids used in this research.

The generality of this mechanism could also be studied. In this study, only one quantum dot composition and one quantum dot size was used. The exact composition of the quantum dot used in this study was not known, but again it was assumed to be a CdSe core with a ZnS shell. Other possible quantum dot chemistries such as cadmium telluride, zinc cadmium sulfide, or

cadmium free quantum dots such as $CuInS_2$ could be also be investigated[16]. Some testing with other quantum dot size was done, but only sparingly and no conclusive results were determined. It would be interesting to see if the band gap energy affects the mechanism for electroluminescence.

Finally, it would be interesting to see if quantum dots are a necessary component of the mechanism or can any semiconducting material function as the emissive layer in this device architecture.

References

[1] Bae, Wan Ki, Sergio Brovelli, and Victor I. Klimov. "Spectroscopic Insights into the Performance of Quantum Dot Light-Emitting Diodes." *MRS Bulletin* 38.09 (2013): 721-30. Print.

[2] Supran, Geoffrey J., et al. "QLEDs for Displays and Solid-State Lighting." *MRS Bulletin* 38.09 (2013): 703-11. Print.

[3] Sun, Qingjiang, et al. "Bright, Multicoloured Light-Emitting Diodes Based on Quantum Dots." *Nature Photonics* 1.12 (2007): 717-22. Print.

[4] Talapin, Dmitri V., and Jonathan Steckel. "Quantum Dot Light-Emitting Devices." *MRS Bulletin* 38.09 (2013): 685-91. Print.

[5] Campbell, Mikey. "Apple Intensifies Research Into Quantum Dot-Enhanced Displays." February 6, 2014 2014.Web. <http://appleinsider.com/articles/14/02/06/apple-intensifies-research-into-quantum-dot-enhanced-displays>.

[6] Hines, Douglas A., and Prashant V. Kamat. "Recent Advances in Quantum Dot Surface Chemistry." *ACS Applied Materials & Interfaces* (2014). Print.

[7] Wood, Vanessa, et al. "Electroluminescence from Nanoscale Materials Via Field-Driven Ionization." *Nano Letters* 11.7 (2011): 2927-32. Print.

[8] Hapiot, Philippe, and Corinne Lagrost. "Electrochemical Reactivity in Room-Temperature Ionic Liquids." *Chemical reviews* 108.7 (2008): 2238-64. Print.

[9] Visentin, Adam F., and Matthew J. Panzer. "Poly(Ethylene Glycol) Diacrylate-Supported Ionogels with Consistent Capacitive Behavior and Tunable Elastic Response." *ACS Applied Materials & Interfaces* 4.6 (2012): 2836-9. Print.

[10] Shi, Xingbo, et al. "Photobleaching of Quantum Dots by Non-Resonant Light." *Physical Chemistry Chemical Physics* 15.9 (2013): 3130-2. Print.

[11] van Sark, Wilfried G. J. H. M., et al. "Photooxidation and Photobleaching of Single CdSe/ZnS Quantum Dots Probed by Room-Temperature Time-Resolved Spectroscopy." *The Journal of Physical Chemistry B* 105.35 (2001): 8281-4. Print.

[12] Blanck, Harvey F. "Introduction to a Quantum Mechanical Harmonic Oscillator using a Modified Particle-in-a-Box Problem." *Journal of chemical education* 69.2 (1992): 98. Print.

[13] Kippeny, Tadd, Laura A. Swafford, and Sandra J. Rosenthal. "Semiconductor Nanocrystals: A Powerful Visual Aid for Introducing the Particle in a Box." *Journal of chemical education* 79.9 (2002): 1094. Print

[14] Chen, Wei, Dennis Grouquist, and Joel Roark. "Voltage Tunable Electroluminescence of CdTe Nanoparticle Light-Emitting Diodes." [Abstract]. *Journal of nanoscience and nanotechnology* 2.1 (2002): 47-53. Print.

[15] Carroll, John J., John D. Slupsky, and Alan E. Mather. "The Solubility of Carbon Dioxide in Water at Low Pressure." *Journal of Physical and Chemical Reference Data* 20 (1991): 1201. Print.

[16] CRC Handbook. 76th Edition. 1995.

[16] Li, Liang, et al. "Highly Luminescent CuInS2/ZnS Core/Shell Nanocrystals: Cadmium-Free Quantum Dots for in Vivo Imaging." *Chemistry of Materials* 21.12 (2009): 2422-9. Print.

Appendix A

Table 1. Quantum Dot Film Thickness vs. Turn-On Voltage

Thickness (nm)	Turn-On Voltage AC Bias (V PTP)
100	19.7
62.11	9.3
32.6	4.81

Appendix B

One group of testing was on the effect of the ionic liquid on the device performance. After doing a literature search, it was noted that ionic liquids could support the highly reactive O_2^- superoxide species. With this in mind, EMIFAP was chosen because it too was shown to support the superoxide formation and EMITCB was chosen because there was no literature stating it could support the superoxide species. All three of these ionogels were functional. This again suggested that water was most likely the limiting reactant. It did rule out oxygen as a possible reactant because it was possible that EMITCB did support the superoxide ion.

Another test was examining the ionogel precursor solution without curing the solution. A quantum dot coated ITO substrate was held flat and electrical contact was made with the ITO. A small amount precursor solution was placed on the substrate. The circuit was completed by touching a small metal wire to each solution. The precursor solution showed electroluminescence, but was still limited to the triple interface.

Appendix C

a) The original image from Figure 3.2.2 (b)

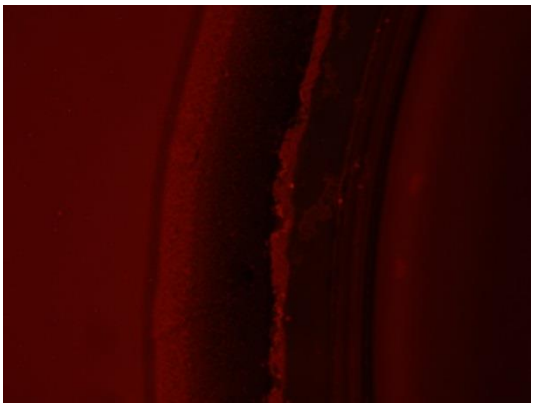

b) Fluorescent Microscope Image of the Photoluminescence of a coplanar device. The magnifaction of this image is 4X.

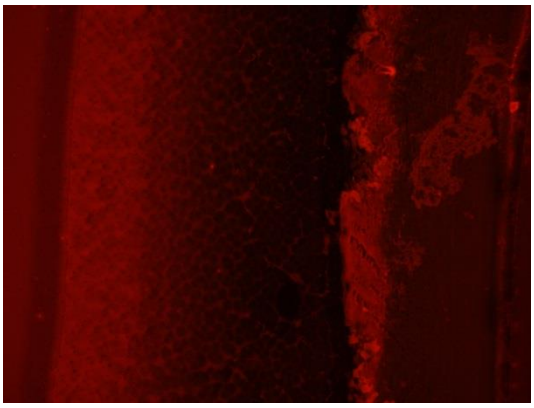

c) Increased Magnification of image (b). This is at the triple interface. The magnifaction of this image is 10X.

Appendix D

The CV testing was performed based on research performed by Katayama et. al. which showed that ionic liquids could stabilize the highly reactive O_2^- species[1]. Katayama et. al. claimed that in a CV sweep, peaks at -1.5V compared to an Ag reference wire were associated with the O_2^- species[1]. This research thought that O_2^- could be a possible product of the redox reaction if oxygen was the main component. A graph of the final cycle in the cyclic voltammetry

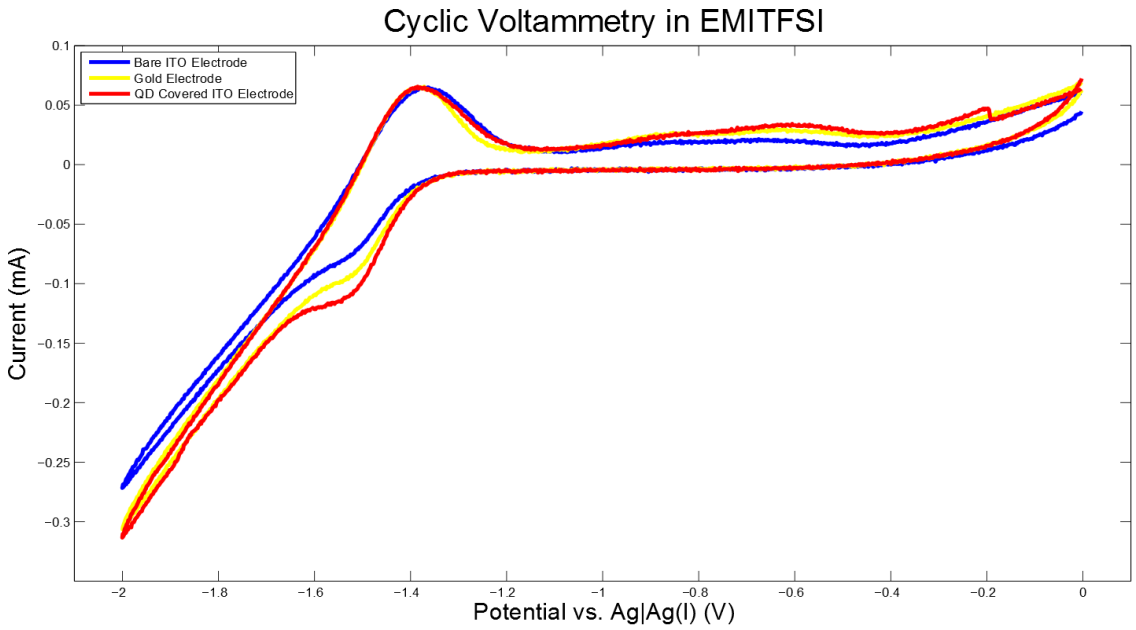

a) Cyclic Voltammetry in EMITFSI. The three different conditions show that the superoxide formation is possible. The sweep rate for this testing was 0.01 V/second.

testing was shown in the Figure above.

This CV agreed with the results from Katayama et. al.[1] This suggested that oxygen was a possible reactant in the redox reaction, but did not decisively demonstrate that oxygen was the only reactant necessary for electroluminescence. Katayama et. al. also suggested that a peak for

[1] Katayama, Yasushi, et al. "Electrochemical Reduction of Oxygen in some Hydrophobic Room-Temperature Molten Salt Systems." *Journal of the Electrochemical Society* 151.1 (2004): A59-63. Print.

water should also have showed up[1]. It was known that EMITFSI in ambient conditions did contain some water, but no peak was visible in this testing. One explanation suggested that the water peak was touching the superoxide peak. This accounted for the fact that no isolated water peak was seen.

Appendix E

Another possible explanation for the increased electroluminescence when devices were exposed to steam was the increased temperature. The increased temperature could have increased the reaction rate and increased the amount of electroluminescence. The same setup as the boiling water setup was tested, except instead of exposing the triple interface to the vapor, the glass substrate side was exposed. This was shown to decrease the amount of electroluminescence seen. In order to remove the steam from the experiment, a heat gun was used. The head gun was used on a functional device, and the performance decreased again. This confirmed that something in the vapor phase was the key to the redox reaction.

Appendix F

Matlab code to find the peaks from the stability data:

```
% This function removes any non-peak data and plots the data as a scatter plot
% Photodata is the raw data with the first column being the time and the second column
%           being the intensity

function RemoveUncessaryData(photoData)

    % Gets the first and the third points
    previous = photoData(1,2);
    next = photoData(3,2);
    temp = 1;

   % Goes through all of the data
    for i = 2:length(photoData)-2

        % If the intensity of the current position is greater than the previous and greater than the next
        % data point, it gets added to photoDataEdit1
        if (photoData(i,2)>previous && photoData(i,2)>next)
            photoDataEdit1(temp,1) = photoData(i,1);
            photoDataEdit1(temp,2) = photoData(i,2);
            temp = temp + 1;
        end
        previous = photoData(i,2);
        next = photoData(i+2,2);

    end

    % Plots PhotoDatEdit1 as a scatter plot with * markers.  It also labels the axes, and title
    figure(3)
    photoDataEdit1(:,1) = photoDataEdit1(:,1) / 1000;
    scatter(photoDataEdit1(:,1),photoDataEdit1(:,2),'*');
    xlabel('Time (sec)','FontSize',16);
    ylabel('Power (nW)','FontSize',16);
    title('AC Stability','FontSize',20);

end
```

Appendix G

```
% This function fits the PLBase and ELBase data to a single term Gaussian curve
% Wavelengths is the x values that correspond to PLBase and ELBase as the y values
% This function plots the fitted data normalized to 1 and returns the data describing how good of a fit it %   is in Gs
function Gs = ELandPLOverlay(wavelengths,PLBase,ELBase)

    % Fits the data to a Gaussian curve
    [PLFit, G1] = fit(wavelengths,PLBase,'gauss1');
    [ELFit, G2] = fit(wavelengths,ELBase,'gauss1');

    % Evaluates the fit at the same wavelengths the raw data was given at
    plFitData = feval(PLFit,wavelengths);
    elFitData = feval(ELFit,wavelengths);

    % Normalizes the fitted data to 1 by dividing by the maximum of the data
    plFitNorm = plFitData/max(plFitData);
    elFitNorm = elFitData/max(elFitData);
     plnorm = PLBase/max(plFitData);
    elnorm = ELBase/max(elFitData);

    % Plots the fitted data normalized to 1.  Labels the axes and the title.  Also sets the legend
    figure(1);
    scatter(wavelengths,elnorm,20,'r');
    hold on;
    scatter(wavelengths,plnorm,20,'b');
    set(gca,'FontSize',14);
    xlabel('Wavelength (nm)','FontSize',18);
    ylabel('Intensity (a.u.)','FontSize',18);
    title('Normalized Spectra','FontSize',20);
    xlim([500 700]);
    legend('EL','PL');
    legend('Location','NorthWest');

   % Sets the variable to be returned.
    Gs = [G1 G2];

end
```